


Cite this: *RSC Adv.*, 2020, **10**, 17951

Received 27th December 2019  
Accepted 30th April 2020

DOI: 10.1039/c9ra10962e  
rsc.li/rsc-advances

## Synergetic catalysis of a cobalt-based coordination polymer for selective visible-light driven $\text{CO}_2$ -to-CO conversion†

Sheng-Jie Li, Yong-Bin Chang, Ming Li, You-Xiang Feng and Wen Zhang \*

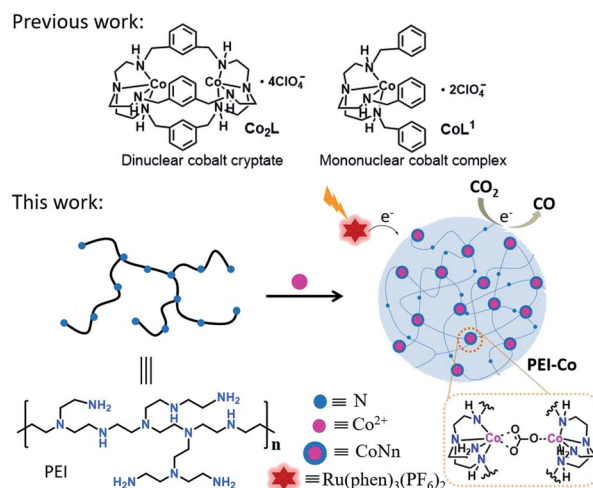
Herein, based on the strategy of synergetic catalysis, we report a cobalt-based coordination polymer  $\text{PEI}_6\text{-Co}$ . As a heterogeneous catalyst,  $\text{PEI}_6\text{-Co}$  shows a selectivity of 95% and a yield of  $1170 \text{ mmol g}^{-1}$  for visible-light-driven  $\text{CO}_2$ -to-CO conversion in a water containing system, which is almost 2.8 times that of the mononuclear cobalt catalyst  $\text{CoL}^1$  and is comparable to that of the dinuclear cobalt catalyst  $\text{Co}_2\text{L}$ .

Energy shortages and greenhouse gas emissions caused by the consumption of fossil fuels have become an indisputable obstacle to the sustainable development of human beings. Solar-driven conversion of  $\text{CO}_2$  to carbon fuels is regarded as an ideal strategy to deal with these energy and environmental issues.<sup>1–7</sup> In this context, many researchers have devoted themselves to promote the activity and efficiency of photocatalytic  $\text{CO}_2$  conversion.<sup>8–11</sup> Unlike the reduction of  $\text{H}_2\text{O}$  to  $\text{H}_2$ , the  $\text{CO}_2$  reduction reactions are more complicated. Firstly,  $\text{CO}_2$  is an inert molecule, it requires high energy to be activated. Secondly, as the carbon atom in  $\text{CO}_2$  is the highest valence, various reduction products including  $\text{CO}$ ,<sup>12</sup> formic acid,<sup>13</sup> formaldehyde,<sup>14</sup> methane<sup>15</sup> and some multi-carbon products<sup>16</sup> can be obtained. Besides, due to the competitive reduction of protons, the selectivity of  $\text{CO}_2$  reduction is usually low in water containing medium.<sup>17</sup> In this context, the development of a catalyst for the efficient and highly selective reduction of  $\text{CO}_2$  to a single valuable product is still challenging, especially in water containing system.

In recent decades, many molecular catalysts for the reduction of  $\text{CO}_2$  have been designed elaborately. For example, the catalysts based on Ru,<sup>18,19</sup> Re,<sup>20,21</sup> Ir,<sup>22</sup> Fe,<sup>23,24</sup> Co,<sup>25,26</sup> Ni,<sup>27,28</sup> Mn,<sup>29</sup> etc., have been developed to reduce  $\text{CO}_2$  and the mechanisms for the activation and conversion of  $\text{CO}_2$  have also been investigated reasonably.<sup>30,31</sup> Notable among them is dinuclear metal synergistic catalysis (DMSC) in which two active centers are involved into the catalytic reaction concurrently and used to decrease the reaction barriers.<sup>32–34</sup> In our previous works,<sup>25</sup> dinuclear cobalt cryptate  $\text{Co}_2\text{L}$  (Scheme 1) which was composed of aza-cryptand ligand and two adjacent cobalt ions displayed

excellent performance in the conversion of  $\text{CO}_2$  to CO. Due to the immobilization and synergistic catalysis of two adjacent cobalt active sites to  $\text{CO}_2$  molecules, the selectivity and the turnover numbers (TON) of  $\text{Co}_2\text{L}$  reached as high as 98%, and 16 896, respectively. Although molecular catalysts are significant in the study of catalytic mechanism and optimizing catalyst structure, the synthesis operations of such molecular catalyst are tedious and not conducive to its large-scale practical applications.

Herein, we choose polyethyleneimine (PEI) as the analogue of aza-cryptand and synthesize a cobalt-based coordination polymer ( $\text{PEI}_6\text{-Co}$ ) as a heterogeneous catalyst for the photocatalytic reduction of  $\text{CO}_2$  (Scheme 1). The reason for choosing PEI as a ligand is that both the structures of aza-cryptand and PEI have secondary amine and tertiary amine groups which can coordinate with  $\text{Co}^{2+}$ . The formation of the coordination polymer can shorten the distance between cobalt active sites, which



Scheme 1 The structures of  $\text{Co}_2\text{L}$ ,  $\text{CoL}^1$ ,  $\text{PEI}_6\text{-Co}$  and the proposed catalysis process of  $\text{PEI}_6\text{-Co}$  for  $\text{CO}_2$ -to-CO conversion.

MOE International Joint Laboratory of Materials Microstructure, Institute for New Energy Materials and Low Carbon Technologies, School of Material Science and Engineering, Tianjin University of Technology, Tianjin 300384, China. E-mail: zhangwen@email.tjut.edu.cn

† Electronic supplementary information (ESI) available: Including XPS, CV, HRMS (ESI), UV absorption spectrum. See DOI: 10.1039/c9ra10962e



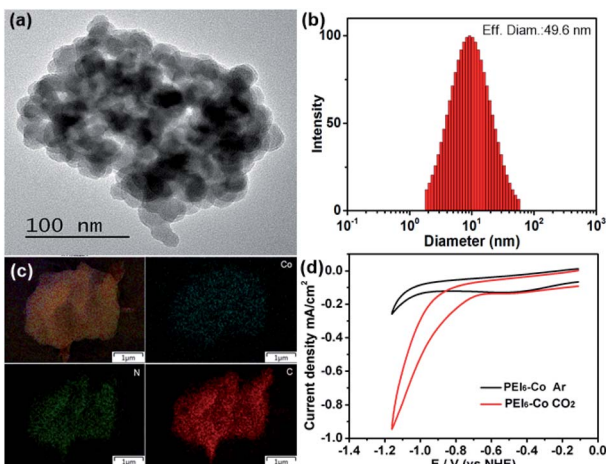


Fig. 1 (a) TEM image of  $\text{PEI}_6\text{-Co}$ . (b) DLS data of  $\text{PEI}_6\text{-Co}$ . (c) Mapping images of  $\text{PEI}_6\text{-Co}$ . (d) CV curves of  $\text{PEI}_6\text{-Co}$  in  $\text{CH}_3\text{CN}/\text{H}_2\text{O}$  (4 : 1) solution under an Ar (black) and  $\text{CO}_2$  atmosphere (red) at 25 °C.

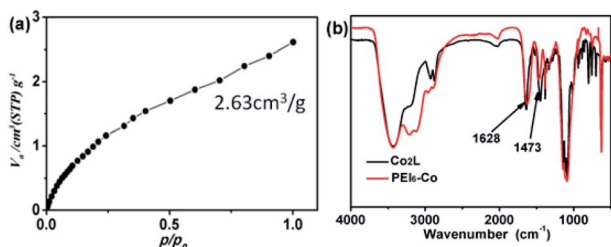


Fig. 2 (a) The adsorption curve for carbon dioxide of  $\text{PEI}_6\text{-Co}$ . (b) IR spectra of  $\text{PEI}_6\text{-CO}$  (red) and  $\text{Co}_2\text{L}$  (black) after adsorption of  $\text{CO}_2$ .

Table 1 Comparison of photocatalytic carbon dioxide reduction of  $\text{PEI}_x\text{-Co}^a$

Entry	Catalyst	$n_{\text{H}_2}$ (μmol)	$n_{\text{CO}}$ (μmol)	Selectivity of CO	Activity (mmol g <sup>-1</sup> )
1	$\text{PEI}_4\text{-Co}$	0.35	4.35	93%	870
2	$\text{PEI}_5\text{-Co}$	0.36	4.71	93%	942
3	$\text{PEI}_6\text{-Co}$	0.34	5.84	95%	1170
4	$\text{PEI}_7\text{-Co}$	0.30	5.09	96%	1020
5	$\text{PEI}_8\text{-Co}$	0.26	4.90	95%	981

<sup>a</sup> Reaction conditions:  $\text{PEI}_x\text{-Co}$  (5 μg),  $[\text{Ru}(\text{phen})_3](\text{PF}_6)_2$  (0.4 mM), TEOA (0.3 M), 5 mL  $\text{CH}_3\text{CN}/\text{H}_2\text{O}$  (v/v = 4 : 1) solution, 25 °C, 12 h, 450 nm LED lamp (100 mW cm<sup>-2</sup>, irradiation area 0.8 cm<sup>2</sup>).

is similar to that of  $\text{Co}_2\text{L}$ , so that they may function synergistically in the photocatalytic reactions. Besides, PEI has been commonly used as a  $\text{CO}_2$  absorbent in the past research of electrocatalytic reduction of  $\text{CO}_2$ .<sup>35</sup> As a result, when  $\text{PEI}_6\text{-Co}$  is used as a heterogeneous catalyst for the reduction of  $\text{CO}_2$  in water containing system, the selectivity for CO reaches up to 95%, and the yield for  $\text{CO}_2$ -to-CO conversion reaches 1170 mmol g<sup>-1</sup>, which is almost 2.8 times of molecular catalyst mononuclear cobalt  $\text{CoL}^1$  and comparable with that of dinuclear cobalt catalyst  $\text{Co}_2\text{L}$ .

$\text{Co}_2\text{L}$  and  $\text{CoL}^1$  were prepared according to the literature.<sup>25</sup>  $\text{PEI}_x\text{-Co}$  ( $x$  represents the N/Co ratio) was synthesized through the coordination between the amine groups of PEI and cobalt ions and the exact contents of cobalt in the catalyst are listed in Table S1 (see ESI†). At the beginning, the formation of  $\text{PEI}_6\text{-Co}$  was characterized by TEM, DLS, element mapping, XPS and cyclic voltammetry measurements. As shown in Fig. 1a,  $\text{PEI}_6\text{-Co}$  was formed as a nanoparticle which resulted from the coordination crosslinking between the amino groups of PEI and Co ions. DLS measurement in Fig. 1b shows that the average diameter of this nanocomposite is about 50 nm. The elemental mapping images confirm that the Co, N and C elements uniformly distributed over the nanostructures of  $\text{PEI}_6\text{-Co}$  (Fig. 1c). The XPS measurement shows that there are only Co, N, C, O and Cl element in  $\text{PEI}_6\text{-Co}$  (Fig. S1†). These results indicate that amine groups in the PEI chain can coordinate with the cobalt ions, causing the long chain of the PEI to be twisted and crosslinked to form nanoparticles and giving the chance for cobalt centers to get closer. Besides, the redox property of  $\text{PEI}_6\text{-Co}$  was investigated using cyclic voltammogram (CV). The results in Fig. 1d show that compared with the CV curve under argon condition, the current has an obvious enhancement under  $\text{CO}_2$  atmosphere and the onset potential ( $E_{\text{onset}} = -0.62$  V vs. NHE) is more negative than that of  $\text{Co}_2\text{L}$  ( $E_{\text{onset}} = -0.68$  V vs. NHE, Fig. S2†) and  $\text{CoL}^1$  ( $E_{\text{onset}} = -0.76$  V vs. NHE, Fig. S3†), indicating that  $\text{PEI}_6\text{-Co}$  can reduce  $\text{CO}_2$  more easily than  $\text{Co}_2\text{L}$  and  $\text{CoL}^1$ . Besides, the redox potential of photosensitizer  $[\text{Ru}(\text{phen})_3]^{3+/2+*}$  was reported as -0.84 V vs. NHE,<sup>26</sup> which is more negative than the onset potential of  $\text{PEI}_6\text{-Co}$  to  $\text{CO}_2$  reduction, thus, it is feasible for  $[\text{Ru}(\text{phen})_3](\text{PF}_6)_2$  to donate electrons to  $\text{PEI}_6\text{-Co}$  under light irradiation, which is one of the foundations for driving the reduction of  $\text{CO}_2$ .

In addition, to examine the gathering ability of  $\text{PEI}_6\text{-Co}$  to  $\text{CO}_2$ ,  $\text{CO}_2$  adsorption experiment was carried out. As shown in Fig. 2a,  $\text{PEI}_6\text{-Co}$  has an adsorption capacity of 2.63 cm<sup>3</sup> g<sup>-1</sup> towards  $\text{CO}_2$ . The IR spectra in Fig. 2b shows that after the treatment of  $\text{CO}_2$  atmosphere, both  $\text{PEI}_6\text{-Co}$  and  $\text{Co}_2\text{L}$  have two peaks at 1628 cm<sup>-1</sup> and 1473 cm<sup>-1</sup>, which belong to the stretching vibrations of the carbonate group. All these results indicate that  $\text{PEI}_6\text{-Co}$ , just like the molecular catalyst binuclear cobalt  $\text{Co}_2\text{L}$ , has the ability of adsorbing  $\text{CO}_2$ , which is favorable for the reduction of  $\text{CO}_2$  in the heterogeneous catalysis process.

Encouraged by the positive results above, we optimized the atom ratio of N and Co in the catalysts for the reduction of  $\text{CO}_2$ . In the photoreaction system, the reaction solutions were prepared by adding photocatalyst  $\text{PEI}_x\text{-Co}$  and photosensitizer  $[\text{Ru}(\text{phen})_3](\text{PF}_6)_2$  to  $\text{CH}_3\text{CN}/\text{H}_2\text{O}$  (v/v = 4 : 1) solutions with triethanolamine (TEOA) as a reducing agent. The quartz reaction bottle was sealed by the rubber tube and filled with  $\text{CO}_2$  for 30 min, then, followed by the irradiation of a 450 nm LED light. With the increase of N/Co ratio in the catalyst, the yield of CO product shows a volcano-type trend (Table 1). The highest yield of 1170 mmol g<sup>-1</sup> for CO is achieved when the ratio between N and Co reaches 6 : 1. This result indicates that the appropriate coordination structure is feasible for the reduction of  $\text{CO}_2$ . When the ratio of N/Co is low (entries 1 and 2), the uncoordinated N atoms is insufficient to adsorb  $\text{CO}_2$ . While too



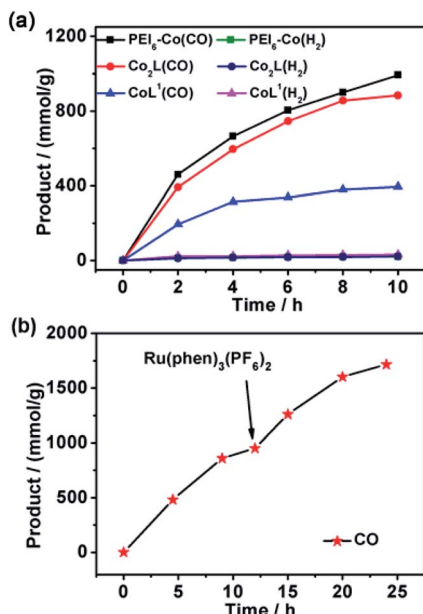


Fig. 3 (a) Comparison of photocatalytic carbon dioxide reduction yield of PEI<sub>6</sub>-Co Co<sub>2</sub>L and CoL<sup>1</sup>. (b) Stability test of PEI<sub>6</sub>-CO.

Table 2 Photocatalytic carbon dioxide reduction control experiment of PEI<sub>6</sub>-CO

Entry	<i>n</i> <sub>H<sub>2</sub></sub> (μmol)	<i>n</i> <sub>CO</sub> (μmol)	Selectivity of CO (%)	Activity (mmol g <sup>-1</sup> )
1 <sup>a</sup>	0	0.17	100%	34
2 <sup>b</sup>	0	0	—	0
3 <sup>c</sup>	0	0	—	0
4 <sup>d</sup>	0	0	—	0
5 <sup>e</sup>	0	0	—	0
6	0.34	5.84	95%	1170

<sup>a</sup> No PEI<sub>6</sub>-Co. <sup>b</sup> No TEOA. <sup>c</sup> No photosensitizer. <sup>d</sup> No light. <sup>e</sup> 100% Ar.

much N atoms would saturate the cobalt center and prevent it from acting as an active center to catalyze CO<sub>2</sub> reduction (entries 4 and 5). Besides, in the liquid phase, only trace amount of formate ( $\sim 0.4$  μmol) was detected by ion chromatograph (Fig. S4†). In addition, photoreactions with different catalyst dosage show that the production of CO is a first order dependence on the concentration of PEI<sub>6</sub>-Co (Fig. S5†).

To investigate the synergistic catalysis effect of PEI<sub>6</sub>-Co, the reported dinuclear cobalt cryptate Co<sub>2</sub>L and mononuclear cobalt CoL<sup>1</sup> complex were chosen as the counterpoints and the photoreactions were carried out under similar conditions (the amount of Co ion was kept same in these catalysts). As shown in Fig. 3a, for PEI<sub>6</sub>-Co, the CO product increased nonlinearly under the visible light irradiation, giving an activity of 1170 mmol g<sup>-1</sup> for CO<sub>2</sub>-to-CO conversion (Fig. 3a, black line). This value is almost 2.8 times of mononuclear cobalt catalyst CoL<sup>1</sup> (416 mmol g<sup>-1</sup>, Fig. 3a, blue line) and comparable with dinuclear cobalt catalyst Co<sub>2</sub>L (884 mmol g<sup>-1</sup>, Fig. 3a, red line), indicating that the easy-to-synthesized coordination polymer

can also achieve the efficient reduction of CO<sub>2</sub> as elaborate molecular catalyst. It is worth noting that when the reaction time reaches 6 h, the evolution rate of CO slows down and even stop. We speculate that the instability of photosensitizer may be a cause of the reaction stopping. Thus we investigate the stability of [Ru(phen)<sub>3</sub>](PF<sub>6</sub>)<sub>2</sub> before and after the photoreaction using mass spectrometry. The results in Fig. S6 and S7† show that one phenanthroline ligand is substituted by two H<sub>2</sub>O molecule after 10 h light irradiation and form [Ru(phen)<sub>2</sub>(H<sub>2</sub>O)<sub>2</sub>](PF<sub>6</sub>)<sub>2</sub>, which has no effect for CO<sub>2</sub> reduction as photosensitizer. In addition, the tracking of UV-visible absorption spectrum of [Ru(phen)<sub>3</sub>](PF<sub>6</sub>)<sub>2</sub> shows that the absorbance of [Ru(phen)<sub>3</sub>](PF<sub>6</sub>)<sub>2</sub> decreases with the light irradiation (Fig. S8†). These results suggest that [Ru(phen)<sub>3</sub>](PF<sub>6</sub>)<sub>2</sub> decomposed with the light irradiation. In addition, we performed a cyclic stability test on the reaction system by re-adding the photosensitizer [Ru(phen)<sub>3</sub>](PF<sub>6</sub>)<sub>2</sub> to the stopped photoreactor. The results in Fig. 3b show that with the addition of extra [Ru(phen)<sub>3</sub>](PF<sub>6</sub>)<sub>2</sub>, the photoreaction could restart and the evolution rate of CO is almost maintained, which suggests that the decomposition of [Ru(phen)<sub>3</sub>](PF<sub>6</sub>)<sub>2</sub> is the main fact for the reduced rate of CO evolution while PEI<sub>6</sub>-Co is relatively stable as a photocatalyst for CO<sub>2</sub> conversion in water containing system.

To illustrate the role of each component in the photoreaction, a sequence of control experiments were carried out (Table 2). In the absence of PEI<sub>6</sub>-Co, a little amount of CO generated (Table 2, entry 1), indicating that PEI<sub>6</sub>-Co was significant to drive the reduction of CO<sub>2</sub> and [Ru(phen)<sub>3</sub>](PF<sub>6</sub>)<sub>2</sub> could catalyze the conversion of CO<sub>2</sub>-to-CO weakly. Further control experiments suggested that the existence of [Ru(phen)<sub>3</sub>](PF<sub>6</sub>)<sub>2</sub>, TEOA, and light was indispensable for the generation of CO (Table 2, entries 2–4). Additionally, when Ar was used as the substitution of CO<sub>2</sub> (Table 2, entries 5), no CO was detected in the photocatalytic system, indicating that the producing of CO was originated from the reduction of CO<sub>2</sub> instead of other organic components.

## Conclusions

In summary, based on the synergic catalytic strategy of dinuclear cobalt, we designed and synthesized a transition metal coordination polymer PEI<sub>6</sub>-Co and investigated its catalytic activity towards CO<sub>2</sub> reduction. The results show that because of the effective adsorption of CO<sub>2</sub> by PEI and the synergic catalytic effect of the adjacent cobalt active sites in PEI<sub>6</sub>-Co, the conversion of CO<sub>2</sub>-to-CO with high yield of 1170 mmol g<sup>-1</sup> and selectivity of 95% were achieved in water containing medium. Such performance is almost 2.8 times of mononuclear cobalt catalyst CoL<sup>1</sup> and comparable with dinuclear cobalt catalyst Co<sub>2</sub>L. This work provides a prospective strategy for the transformation of molecular catalyst to heterogeneous catalyst in a convenient and cost-effective way.

## Conflicts of interest

There are no conflicts to declare.



## Acknowledgements

This work was financially supported by NSFC (21702146) and Natural Science Foundation of Tianjin (19JCQNJC05500).

## Notes and references

- 1 S. Chen, Y. Qi, C. Li, K. Domen and F. Zhang, *Joule*, 2018, **2**, 2260–2288.
- 2 J. Jian, G. Jiang, R. van de Krol, B. Wei and H. Wang, *Nano Energy*, 2018, **51**, 457–480.
- 3 D. Kim, K. K. Sakimoto, D. Hong and P. Yang, *Angew. Chem., Int. Ed.*, 2015, **54**, 3259–3266.
- 4 A. K. Singh, J. H. Montoya, J. M. Gregoire and K. A. Persson, *Nat. Commun.*, 2019, **10**, 443.
- 5 H. Tong, S. Ouyang, Y. Bi, N. Umezawa, M. Oshikiri and J. Ye, *Adv. Mater.*, 2012, **24**, 229–251.
- 6 C. Gao, Q. Meng, K. Zhao, H. Yin, D. Wang, J. Guo, S. Zhao, L. Chang, M. He, Q. Li, H. Zhao, X. Huang, Y. Gao and Z. Tang, *Adv. Mater.*, 2016, **28**, 6485–6490.
- 7 T. Arai, S. Sato and T. Morikawa, *Energy Environ. Sci.*, 2015, **8**, 1998–2002.
- 8 S. N. Habisreutinger, L. Schmidt-Mende and J. K. Stolarczyk, *Angew. Chem., Int. Ed.*, 2013, **52**, 7372–7408.
- 9 D. C. Grills and E. Fujita, *J. Phys. Chem. Lett.*, 2010, **1**, 2709–2718.
- 10 K. Li, B. Peng and T. Peng, *ACS Catal.*, 2016, **6**, 7485–7527.
- 11 X. Li, J. Yu, M. Jaroniec and X. Chen, *Chem. Rev.*, 2019, **119**, 3962–4179.
- 12 Q.-Q. Bi, J.-W. Wang, J.-X. Lv, J. Wang, W. Zhang and T.-B. Lu, *ACS Catal.*, 2018, **8**, 11815–11821.
- 13 S. Gao, Y. Lin, X. Jiao, Y. Sun, Q. Luo, W. Zhang, D. Li, J. Yang and Y. Xie, *Nature*, 2016, **529**, 68.
- 14 P. S. Nabavi Zadeh, M. Zeggi do Valle Gomes, B. Åkerman and A. E. C. Palmqvist, *ACS Catal.*, 2018, **8**, 7251–7260.
- 15 L.-Y. Wu, Y.-F. Mu, X.-X. Guo, W. Zhang, Z.-M. Zhang, M. Zhang and T.-B. Lu, *Angew. Chem., Int. Ed.*, 2019, **58**, 9491–9495.
- 16 H. Jung, S. Y. Lee, C. W. Lee, M. K. Cho, D. H. Won, C. Kim, H.-S. Oh, B. K. Min and Y. J. Hwang, *J. Am. Chem. Soc.*, 2019, **141**, 4624–4633.
- 17 J. L. White, M. F. Baruch, J. E. Pander, Y. Hu, I. C. Fortmeyer, J. E. Park, T. Zhang, K. Liao, J. Gu, Y. Yan, T. W. Shaw, E. Abelev and A. B. Bocarsly, *Chem. Rev.*, 2015, **115**, 12888–12935.
- 18 R. Kuriki, H. Matsunaga, T. Nakashima, K. Wada, A. Yamakata, O. Ishitani and K. Maeda, *J. Am. Chem. Soc.*, 2016, **138**, 5159–5170.
- 19 R. Kuriki, M. Yamamoto, K. Higuchi, Y. Yamamoto, M. Akatsuka, D. Lu, S. Yagi, T. Yoshida, O. Ishitani and K. Maeda, *Angew. Chem., Int. Ed.*, 2017, **56**, 4867–4871.
- 20 T. Morimoto, T. Nakajima, S. Sawa, R. Nakanishi, D. Imori and O. Ishitani, *J. Am. Chem. Soc.*, 2013, **135**, 16825–16828.
- 21 T. Morimoto, C. Nishiura, M. Tanaka, J. Rohacova, Y. Nakagawa, Y. Funada, K. Koike, Y. Yamamoto, S. Shishido, T. Kojima, T. Saeki, T. Ozeki and O. Ishitani, *J. Am. Chem. Soc.*, 2013, **135**, 13266–13269.
- 22 S. Sato, T. Morika, T. Kajino and O. Ishitani, *Angew. Chem., Int. Ed.*, 2013, **52**, 988–992.
- 23 C. Cometto, R. Kuriki, L. Chen, K. Maeda, T.-C. Lau, O. Ishitani and M. Robert, *J. Am. Chem. Soc.*, 2018, **140**, 7437–7440.
- 24 P. G. Alsabeh, A. Rosas-Hernandez, E. Barsch, H. Junge, R. Ludwig and M. Beller, *Catal. Sci. Technol.*, 2016, **6**, 3623–3630.
- 25 T. Ouyang, H.-H. Huang, J.-W. Wang, D.-C. Zhong and T.-B. Lu, *Angew. Chem., Int. Ed.*, 2017, **56**, 738–743.
- 26 T. Ouyang, H.-J. Wang, H.-H. Huang, J.-W. Wang, S. Guo, W.-J. Liu, D.-C. Zhong and T.-B. Lu, *Angew. Chem., Int. Ed.*, 2018, **57**, 16480–16485.
- 27 V. S. Thoi, N. Kornienko, C. G. Margarit, P. Yang and C. J. Chang, *J. Am. Chem. Soc.*, 2013, **135**, 14413–14424.
- 28 C. Zhao, X. Dai, T. Yao, W. Chen, X. Wang, J. Wang, J. Yang, S. Wei, Y. Wu and Y. Li, *J. Am. Chem. Soc.*, 2017, **139**, 8078–8081.
- 29 E. Torralba-Peñalver, Y. Luo, J.-D. Compain, S. Chardon-Noblat and B. Fabre, *ACS Catal.*, 2015, **5**, 6138–6147.
- 30 H. Takeda, K. Koike, H. Inoue and O. Ishitani, *J. Am. Chem. Soc.*, 2008, **130**, 2023–2031.
- 31 W. Kubo and T. Tatsuma, *J. Am. Chem. Soc.*, 2006, **128**, 16034–16035.
- 32 L. Zong, C. Wang, A. M. P. Moeljadi, X. Ye, R. Ganguly, Y. Li, H. Hirao and C.-H. Tan, *Nat. Commun.*, 2016, **7**, 13455.
- 33 N. P. Mankad, *Chem. – Eur. J.*, 2016, **22**, 5822–5829.
- 34 A. Magnusson, M. Anderlund, O. Johansson, P. Lindblad, R. Lomoth, T. Polivka, S. Ott, K. Stensjo, S. Styring, V. Sundstrom and L. Hammarstrom, *Acc. Chem. Res.*, 2009, **42**, 1899–1909.
- 35 S. Zhang, P. Kang, S. Ubnoske, M. K. Brennaman, N. Song, R. L. House, J. T. Glass and T. J. Meyer, *J. Am. Chem. Soc.*, 2014, **136**, 7845–7848.

